Sensors & Actuators: B. Chemical 355 (2022) 131276

Contents lists available at ScienceDirect

Sensors and Actuators: B. Chemical

journal homepage: www.elsevier.com/locate/snb

Calibration and field deployment of low-cost sensor network to monitor underground pipeline leakage

Younki Cho [a,*], Kathleen M. Smits [a], Stuart N. Riddick [b], Daniel J. Zimmerle [b]

[a] Department of Civil Engineering, University of Texas Arlington, Arlington, TX, USA
[b] Energy Institute and Department of Mechanical Engineering, Colorado State University, Fort Collins, CO, USA

ARTICLE INFO

Keywords:
Metal oxide semiconductor
Low-cost sensor network
Greenhouse gas
Methane
Natural gas
Underground pipeline leakage

ABSTRACT

Recent technological advances in methane detection have improved leak detection and repair. However, current methods to reliably measure methane concentrations rely on expensive instruments or demand significant labor input. There is interest in using affordable methane sensors that are responsive to ppmv level changes in methane concentrations in both urban and rural environments for monitoring underground natural gas pipeline leaks. This is especially relevant for situations where potentially significant leaks cannot be repaired immediately or smaller leaks that require long-term monitoring and further evaluation. In this work, a low-cost sensor unit, equipped with a metal oxide sensor, was designed, built, and calibrated over a wide range of methane concentrations and environmental conditions in preparation for field application. A network of these sensors was then installed at the test site and used to measure methane concentrations at ground level above known sub-surface natural gas emissions which emulated underground gas pipeline leaks. This low-cost sensor network measured over 4 days total for the two different known leakage rates. Results demonstrate that the sensors can continuously measure relative methane variability for extended periods but require calibration for a wide range of temperature and humidity conditions to properly determine absolute gas (i.e., methane) concentrations. When a regression analysis was conducted to evaluate the effects of meteorological parameters on methane concentration, air temperature and wind speed have strong impacts on the concentration. Overall, the network approach allows improved identification of leak location and monitoring of underground natural gas leaks.

1. Introduction

Methane (CH_4) is the second most abundant anthropogenic greenhouse gas after carbon dioxide (CO_2), and has a global warming potential 86 times greater than that of CO_2 over a 20-year period [1]. Atmospheric CH_4 concentrations continue to increase, predominantly due to anthropogenic activities [1–3]. Anthropogenic CH_4 originates from multiple sources including, but not limited to, enteric fermentation, natural gas systems, landfills, manure management, and coal mining [4,5]. As spatiotemporal variability in CH_4 fluxes is observed under dynamic environmental conditions [6–9], the ability to measure relatively small emission sources is challenging without a large number of continuous direct and local level measurements. However, common methods to measure CH_4 concentrations rely on expensive instruments and/or significant labor. For example, estimates of CH_4 concentration from leaking natural gas (NG) pipelines can be made using aircraft or vehicles equipped with high precision instrumentation [10–12]. Traditional walking surveys demand a significant amount of time and labor and vary greatly in effectiveness depending on weather conditions and surveyor experience. Thus, there is a need for a cost-effective, continuous monitoring system for pipeline leaks at high spatial and temporal resolutions, especially when there is a time lapse between detection and repair.

Low-cost gas sensors (~16 US$ per unit) have emerged as a promising tool for improving the spatial density of gas concentration measurements. These sensors are built to monitor various chemical species including CH_4, carbon dioxide, and nitrogen dioxide. For the detection of CH_4, common techniques include metal oxide semiconductor (MOS) [13–15], electrochemical (EC) [16–18], non-dispersive infrared radiation (NDIR) [19], and photoionization detection [20]. MOS sensors have been evaluated in multiple studies and have demonstrated promising performance [9,13–15,21,22]. Previous MOS studies mainly focused on above ground applications rather than pipeline leakage scenarios. Calibration of sensors installed at 1—2 m above the ground at parts per

* Correspondence to: 416 Yates St. Nedderman Hall # 425, Arlington, TX 76010-1539, USA.
E-mail address: younki.cho@uta.edu (Y. Cho).

https://doi.org/10.1016/j.snb.2021.131276
Received 5 February 2021; Received in revised form 4 December 2021; Accepted 15 December 2021
Available online 17 December 2021

million (ppmv) levels is needed [14,15,23] due to each sensor's response at CH_4 concentrations observed during air quality monitoring (in 2—10 parts per million range). Low-cost sensors have also been applied to monitor concentrations nearby carbon sequestration and enhanced oil recovery sites in remote areas using a wireless mesh network integrated, at selective nodes, into a cellular network [9]. For the case of measuring surface concentrations above pipeline leakage, the concentration range is wider, where it can exceed 10,000 ppmv directly above the leak but fall to 100 ppmv within 10 m of the leak location [24]. In addition, MOS sensors show a significant temperature and relative humidity dependence [14,21,23]. Such dependency has not been previously evaluated at concentrations greater than 1000 ppmv [21,22]. The effects of these parameters must be included in calibration to improve the accuracy of high gas concentration measurements at concentrations exceeding 100 ppmv.

There is interest in the application of a sensitive and affordable CH_4 sensor in both commercial and residential areas for monitoring underground NG pipeline leaks. For example, underground leaks are often detected during periodic surveys, but leak behavior may change between surveys or before repair due to variations in environmental conditions, changes in ground cover, or changes in structures near the leak. In the USA, re-evaluation of existing leaks under current guidance occurs every 1—15 months, depending on hazard potential [25]. Therefore, CH_4 concentration monitoring may be needed to monitor a leak before repair, or the long-term dissipation of high concentrations of gas trapped belowground after repair. In addition, changes in patterns of NG distribution due to the intrusion of water from infiltration (i.e., heavy rain) may trap the gas underground [26] or result in gas migration. This type of event would not be easily detected by surveys [27] but could be detected with the appropriate algorithms linked with continuous monitoring.

The use of low-cost sensors to continuously monitor existing leaks could provide information on the changes in leakage rate, underground gas accumulation, or changes in the leak presentation or location that could signify increased safety risk. However, this type of monitoring has not been investigated or deployed at known belowground leak areas, high-risk leakage locations, or other areas requiring long-term leak monitoring. Additionally, monitoring pipeline leaks in leak detection and repair (LDAR) programs is one method to mitigate fugitive greenhouse gas emissions. Development of a low-cost sensor network to observe the surface expression of subsurface CH_4 leakage behavior presents a widely applicable solution for pipeline LDAR.

This study focuses on development and calibration of a NG detection unit using low-cost sensors and field deployment of prototype units. The performance of the detection unit was evaluated by comparing to a portable cavity ring-down spectroscopy (CRDS) analyzer. A field trial was carried out at the Methane Emission Technology Evaluation Center (METEC) at Colorado State University in Fort Collins, Colorado, USA [28]. The detection of relatively small leaks ($\leq$ 3 LPM) was demonstrated using the low-cost sensor units that monitor the concentration of NG plume near the ground surface over diurnal time scales. The sensor deployment provided a representative picture of local gas concentration. The meteorological data were collected in conjunction with the field deployment of the sensors. The effect of meteorological parameters on gas concentration was investigated to improve understanding how those parameters would impact the ability of the sensors to monitor the leak. This work is widely applicable for providing continuous measurements of NG concentrations to operators for a wide range of leak types and to first responders responding to NG leak incidents.

2. Methods

2.1. Sensor configuration

Low-cost sensor (LCS) units consist of three individual sensors – natural gas, relative humidity/temperature, and absolute pressure – enclosed in a plastic case (Fig. 1A). A MOS sensor (TGS2611-E00, Figaro USA Inc.) used to detect NG was selected due to its low cost, relatively high accuracy, and suitability for measuring CH_4 concentration levels in air [22,29,30]; the sensor has a stated detection range of 500—10,000 ppmv [31]. The MOS sensor was specifically selected for the proposed application. The TGS2611-E00 responds to various gases in addition to CH_4, including ethanol (C_2H_6O), hydrogen (H_2), and iso-butane (C_4H_{10}) [23,31]. When these gases are present, the sensor will respond when CH_4 is not present, resulting in falsely high CH_4 readings. Prolonged exposure to the non-target gases may also cause permanent damage (poisoning) of the sensor [31]. To reduce this impact, the MOS sensor includes a charcoal filter in its housing to reduce interference with alcohol or iso-butane, resulting in highly selective response to CH_4 [31].

Additionally, these interference gases are present at low concentrations in the proposed application. Ethanol concentration is typically in the 1—4 ppbv levels in the atmosphere due to its high solubility in water [32], and removal by dissolution into rainwater and surface waters [33–35]. H_2 occurs naturally in the atmosphere [36] but averages 0.53 ppmv [37]. Iso-butane is emitted from anthropogenic sources including industries and motor vehicles [38], but atmospheric concentrations range from 6 to 33 ppbv [39,40]. In all cases, these non-target gases are present at concentrations that do not have a significant influence on the sensor performance and no risk of poisoning the sensor. In contrast, the sensor responds well to CH_4, the principal component of NG while showing no ill effects from ethane and CO_2, the other major constituents of market NG [41].

The resistance of the sensor (R_s) changes as CH_4 is adsorbed by the sensing material and can be calculated from the voltage (V_c, 5.0 V DC $\pm$ 0.02%) applied across the sensor, the load resistor (R_L, 10.0 kΩ $\pm$ 1%) installed in a circuit, and the sensor signal measured as a change in voltage across the load resistor (V_{RL}) (Eq. 1).

$$R_s = \left(\frac{V_c - V_{RL}}{V_{RL}}\right) R_L \tag{1}$$

The MOS sensor uses tin oxide (SnO_2) as the sensing material [31]. In the presence of the target gas, the amount of oxygen adsorbed on the SnO_2 surface is reduced and results in a decrease in resistance. However, the resistance is also affected by air temperature (T) and relative humidity (RH). In the LCS unit, the temperature and RH were measured using a SHT35-DIS-F2.5KS digital sensor (Sensirion AG). The SHT35-DIS-F2.5KS is accurate to $\pm$ 0.1 °C and $\pm$ 1.5% RH [42]. In addition, recent studies indicate that atmospheric pressure (P) influences gas concentrations [43,44]. The atmospheric pressure was measured by a piezoresistive absolute pressure sensor (LPS25HB, STMicroelectronics) which has an accuracy of $\pm$ 0.01 psi [45]. An Arduino Uno Rev3 microcontroller logged the signals from the sensors and recorded the date and time, air temperature, relative humidity, absolute pressure, and resistance to a microSD card at a frequency of 1 Hz using a real-time clock (RTC) (DS3231, Diymore). The analog voltage across the load resistor was converted by a built-in 10-bit analog-to-digital converter in the microcontroller with 5 V reference and resolution of 0—1023. The analog-to-digital converter has an absolute accuracy of $\pm$ 2 LSB [46]. I^2C protocol in the microcontroller was used for the relative humidity/temperature and pressure sensors. The LCS unit was powered by a 12 V "power over ethernet" (PoE) adapter. A small fan (30 $\times$ 30 $\times$ 7 mm) was installed at the inlet of the case to allow for proper gas exchange across the sensors. Both the inlet and outlet were covered with a fine aluminum wire mesh (14 $\times$ 14 mesh with 1.30 mm opening) to minimize dust intrusion.

2.2. Calibration

Laboratory calibration was performed on a MOS sensor at 3 temperatures (28.5 $\pm$ 0.1, 34.2 $\pm$ 0.3, and 40.6 $\pm$ 0.1 ℃) at 8 gas concentrations (0, 10, 50, 100, 500, 1000, 5000, and 10,000 ppmv) and relative

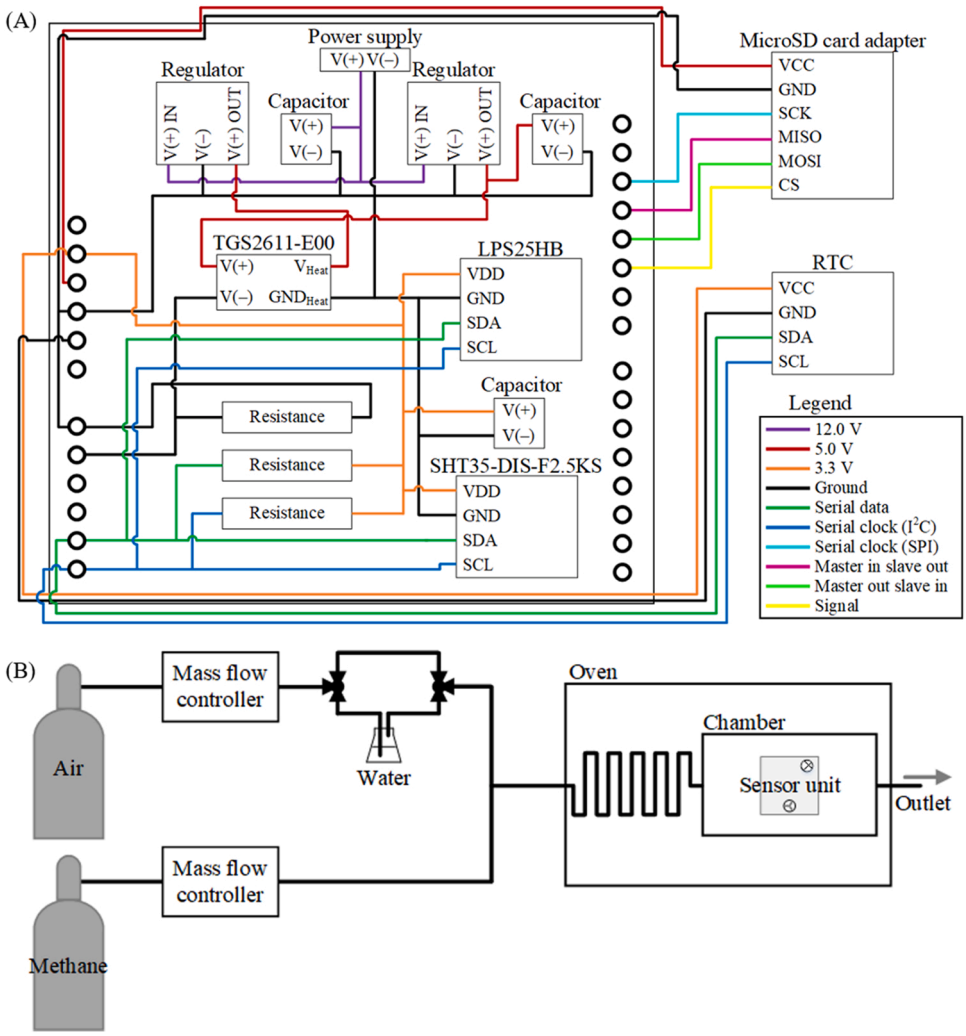

Fig. 1. . (A) A schematic of sensor assembly for a shield board. The shield board sits directly on top of the microcontroller. The assembled board installed on the microcontroller was placed in the case (100 × 100 × 70 mm) to provide protection from water spray and dust. (B) A schematic of the setup used for calibration of the MOS gas sensor (TGS2611-E00).

humidities from 5% to 60% (Fig. 1B). The ranges of temperature and *RH* were selected to represent the field conditions observed at a meteorological station near METEC [47]. Mass flow controllers (MC series, Alicat Scientific) attached to the air and CH_4 gas inlets were used to generate varying gas concentrations in a 2L test chamber. The CH_4 concentration (0—10,000 ppmv) in the chamber was set by directly injecting a mixture of pure gases (i.e., zero grade air and ultra-high purity 99.99% CH_4) blended by the controllers. Because the MOS sensor is relatively insensitive to ethanol and hydrogen compared to CH_4 [31], CH_4 was used for calibration as it is the primary component of NG. Prior to calibration, the test chamber was placed in an oven (Isotemp 650D, Fisher Scientific) to maintain a constant temperature over the calibration period. The oven was started 24 h prior to the experiments. In addition, the sensor unit was preheated for 3 days in ambient air ($CH_4 \leq 2$ ppmv) prior to the calibration to stabilize the MOS sensor. The SHT35-DIS-F2.5KS (air temperature and relative humidity) and LPS25HB (atmospheric pressure) sensors were factory calibrated and were not calibrated onsite.

During calibration, the resistance was measured under varying relative humidity conditions while temperature and gas concentration remained constant. The measured resistance was normalized by the resistance in the ambient air (ambient CH_4 concentration in air (R_o)) to account for any variability between sensors. Calibration results were compared with a cavity ring-down spectrometry analyzer (G4302 GasScouter, Picarro, Inc.). The gas intake for the analyzer was co-located with the LCS units while 100% CH_4 was released from 3 m away at 1 and 2 L min^{-1}. The CH_4 concentrations from the MOS were calculated and compared with the CRDS to assess the efficacy of the calibration algorithm. In addition, *RH* and temperature from SHT35-DIS-F2.5KS were compared to a capacitive thin-film polymer (HUMICAP) sensor (HMP7, Vaisala) under the same calibration conditions to assess performance. SHT35-DIS-F2.5KS and HMP7 were placed in the test chamber at approximately 5 cm apart, and relative humidity in the test chamber was changed from 5% to 60% at 26 ± 0.1 ℃. The HMP7 is designed for applications that involve rapid changes in humidity, such as drying [48] and has an accuracy of ± 0.8%*RH* and ± 0.1 °C [48].

2.3. Field experiments

Field experiments were performed to evaluate the response of the LCS units under the dynamic environmental conditions likely experienced during NG pipeline leak surveillance. Controlled subsurface NG release experiments were conducted at the Colorado State University METEC facility in Fort Collins, Colorado, USA [28]. The site contains pipeline testbeds that vary in configuration, allowing for simulation of underground NG pipeline leaks at known leakage rates using market NG. This study utilized a testbed with a NG emission point located at a depth of 0.91 m below ground surface. The testbed contains natural soil with soil texture classification of sand – a soil type commonly observed

during field operations of local distribution companies. The testbed contains two pipelines: one pipeline located at 0.91 m deep in east-west direction and an additional pipeline at 0.61 m deep in northeast-southwest direction. The testbed was constructed to represent a more complex environment where other utility lines may exist with natural gas pipelines. Emission rate of distribution grade NG (85—87% vol CH_4) from the emission point is controlled by mass flow meters (Omega FMA1700 series) with pressure regulation and solenoid valves [49]. A detailed layout of the testbed can be found in Ulrich et al. [50].

Nineteen LCS units were placed on the ground surface in a radial configuration around the known leakage location (Fig. 2). Spacing and location was selected based on previous experiments that characterized the horizontal extent and concentrations for gas leaks at the selected emission rates [24]. The LCS units were powered on and allowed to equilibrate for 48 h prior to placement around the leak. Data from the LCS units were collected at a frequency of 1 Hz.

Two experiments were carried out over a period of 4 days (2 days per experiment) at CH_4 release rates of 0.042 and 0.127 CH_4 kg h^{-1}. Rates were selected to represent the range of leakage rates observed in the field, typically less than 0.1 kg h^{-1} [10,11,51,52]. In addition to data collected by the LCS units, atmospheric conditions (i.e., wind speed, wind direction, barometric pressure, air temperature, and relative humidity) were monitored using a meteorological station located on site every 1 min.

3. Results

3.1. Calibration

Measured resistance – i.e. observed gas concentration – in the MOS sensor varies with temperature and *RH*. A sample data set shown in Fig. S1A—D (SI Appendix) represents typical responses of measured resistance to *RH* change at a given gas concentration. The air temperature and atmospheric pressure remained constant to within ± 0.4% during all calibration experiments (T = 28.5 ± 0.1 ℃ and P = 99.8 ± 0.1 kPa) as illustrated in Fig. S1C—D. For a given temperature, the resistance of the MOS sensor varies inversely with *RH*.

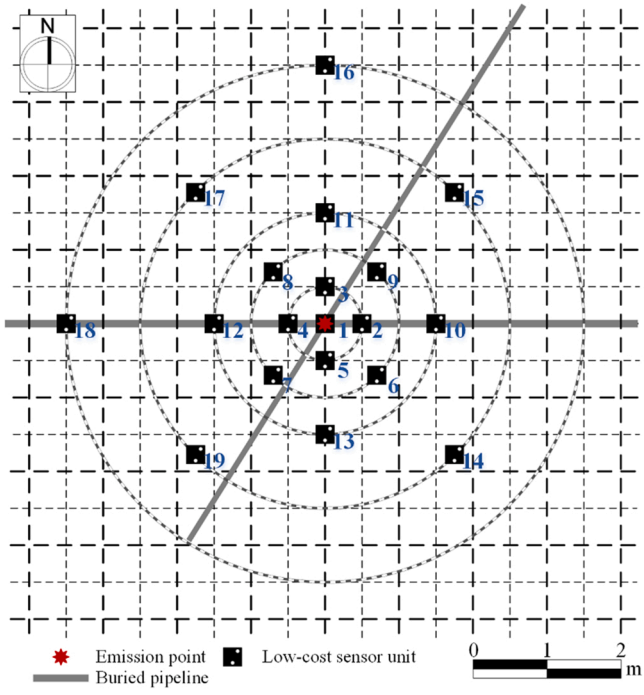

Fig. 2. . Top view schematic of experimental test bed and sensor layout. Sensor units were located on the soil surface while the pipeline and emission point (indicated with the red star) was 0.91 m belowground. The number is assigned next to the corresponding LCS unit. The distances of the LCS units from the emission point are 0, 0.5, 1.0, 1.5, 2.5, and 3.5 m. The figure is drawn to scale.

Measured resistance also dropped systematically with an increase in gas concentration. The results were expressed in terms of normalized resistance (R_s/R_o) in Fig. 3A–C. The effect of temperature on resistance can also be observed, showing a decrease in resistance with an increase in temperature. Multivariate nonlinear regression processing in a series of correlations was selected for data analysis as illustrated in Fig. 4. The relationship between *RH* and R_s/R_o was first described by sigmoid functions at selected temperatures and CH_4 concentrations (Fig. 4A). This information was then used to predict the CH_4 concentration by the R_s/R_o estimated from the *RH* (Fig. 4B). However, it is important to note that the relationship is temperature dependent and therefore each relationship was only applicable to the measured temperatures, in this case, T= 28.5, 34.2, and 40.6 ℃. In order to overcome this constraint, the correlations between CH_4 concentration and temperature were obtained by curve fitting specifically to R_s/R_o and *RH* conditions (Fig. 4C). The range of R_s/R_o(0.01—1.20) for the calibration table was selected based on observations (Fig. 3A—C), and the extreme *RH* conditions (< 5% and > 95%) were not considered. 98% of the coefficient of determination (R^2) was greater than or equal to 0.70.

Calibrations were evaluated by comparing averaged CH_4 concentrations over multiple time intervals (10–150 s at 10 s intervals) to the CRDS analyzer. Averaging over longer time intervals resulted in a better agreement between the MOS sensor and CRDS analyzer; unsurprising since the CRDS has a much faster response rate than the MOS sensor. The response time of the CRDS analyzer is < 1 s while the response time of the MOS sensor was not characterized but was substantially slower. 100-second averaged CH_4 concentrations demonstrated a reasonable level of accuracy; averaging beyond 100 s resulted in no noticeable improvement in agreement (Fig. S2). For subsequent experiments, 100-second averaged data were used for analysis. The differences between the 100-second averaged CH_4 concentration (ΔCH_4) from the two measurements over 120 min at the release rates of 1 and 2 L min^{-1} ranged from 0 to 44 ppmv, averaging 8.3 ppmv with a standard deviation of 6.4 ppmv when all the LCS units were assessed (Fig. S2). Uncertainty in calibration was 12.1 ppmv when one of the calibration functions was evaluated (See SI Appendix). More than 90% of ΔCH_4 was less than or equal to 20 ppmv (Fig. S3).

The more variable CH_4 concentrations seen in the CRDS data (Fig. S4) were due to the faster response rate, as well as higher sensitivity (and accuracy), of the CRDS relative to the MOS sensor. Although there was some discrepancy (0—44 ppmv) between the two measurements, magnitude and trend were well captured using 100-second averaging (Fig. S4). Linear fits (Fig. 5) exhibit near-unity slope (m) (0.99–1.00) with R^2 of 0.85—0.98, after adjusting R_o to obtain better fits to account for the sensor-to-sensor variation between MOS sensors, where R_o ranged from 32—40 kΩ. In the linear fits, the intercepts were forced through the origin. The adjusted R_o, m, and R^2 values of linear regression are listed in Fig. 5. All p-values were less than 0.001. In addition, it was observed that the readings were clustered to a greater extent above the 1:1 line below 100 ppmv and similarly, the readings were clustered below the 1:1 line above 150 ppmv.

It is also important to note that, for the intended application of leak monitoring, precise methane measurements are not required. Since the application focusses on relative change in methane concentration, it is important that measured concentration (a) vary predictably with actual concentrations, and (b) remain stable of a wide range of environmental conditions. Therefore, the calibration results suggest the MOS sensor has suitable performance for estimating CH_4 concentrations above underground leaks.

For the relative humidity/temperature sensor, performance assessment of the SHT35-DIS-F2.5KS was carried out by comparing 100-second averaged data to the HMP7. The results show that difference in

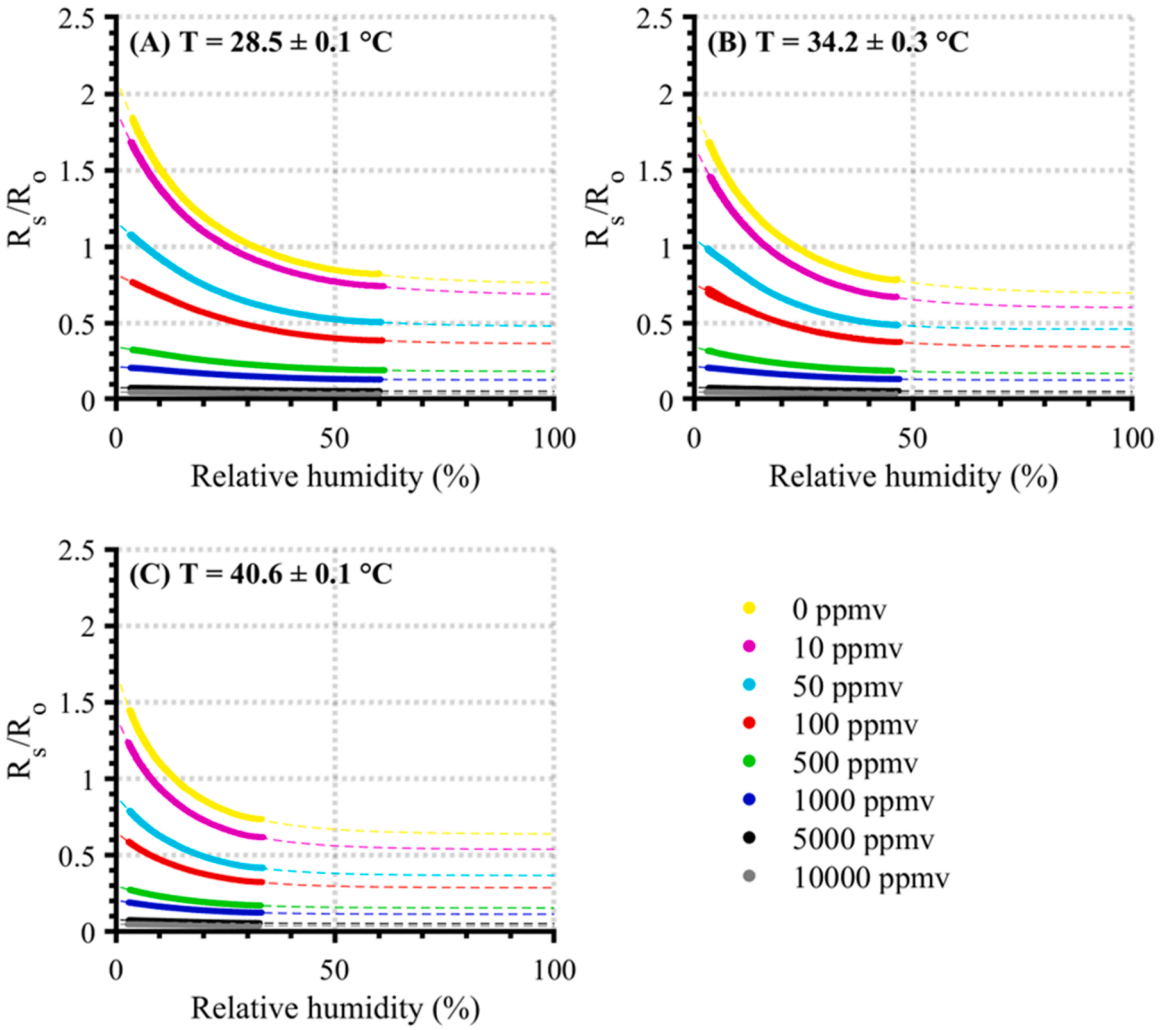

Fig. 3. . R_s/R_o as a function of relative humidity at (A) 28.5 ± 0.1 ℃, (B) 34.2 ± 0.3 ℃, and (C) 40.6 ± 0.1 ℃. The resistance of the ambient air (R_o) was 35.67 kΩ. The dashed lines represent the fitted sigmoid curves to extrapolate the normalized resistance beyond the limit of the measurements (dot symbol). The measured data points are listed in Table S1.

RH was up to 11% (1.8% ± 1.4%, using 1 standard deviation) while maximum difference in temperature was 4 ℃, averaging 1.8 ± 0.7 ℃. When the two sensors were compared (Fig. S4), the linear fits in *RH* were near unity, with R^2 of 0.98—1.00. All p-values were less than 0.001. However, the *RH* from the SHT35-DIS-F2.5KS tends to be lower above 50% RH (range of 0.2–11%, mean 3.5%) (Fig. S5). The temperature measurements from the SHT35-DIS-F2.5KS were consistently higher (+ 1.8 ± 0.7 ℃ in average) than HMP7.

3.2. *Variability in observed methane concentrations during controlled release field experiments*

The 0.042 and 0.127 CH_4 kg h^{-1} controlled release experiments were conducted between the 18th and 22nd of May 2020. Three sensor units (i.e., No. 5, 13, and 15) failed during the 0.042 kg h^{-1} experiment, and two additional units (i.e., No. 11 and 12) failed during the 0.127 kg h^{-1} experiment. The incomplete data collected from these sensors were excluded from the attached data sets and analysis.

During the 0.042 kg h^{-1} experiment, the CH_4 concentration from Sensor No. 1 started at 0.1 ± 0.2 ppmv and increased up to 3112 ± 344 ppmv for the first 29 h of the experiments at which time the gas was shut off (Fig. 6). The CH_4 concentration of Sensor No. 1 gradually decreased back to 24 ± 1 ppmv over the next 19 h. Similarly, for the 0.127 kg h^{-1} experiment, the CH_4 concentration of Sensor No. 1 increased from 0.1 ± 0.2 ppmv to 6112 ± 214 ppmv in 29 h of release and dropped back to 67 ± 2 ppmv after shutoff (Fig. 6B.1).

The results show that in all cases, near-surface CH_4 concentration increased with time after the gas was turned on, reaching quasi steady state approximately 12 h of release. Once at quasi steady state, concentrations continued to vary, but long-duration mean concentrations stabilized. Taking data of Sensor No. 2—4 from the 0.042 kg h^{-1} experiment as an example, after stabilization, the 100-second average readings varied up to 17% of the peak concentrations over the next 12 h (Fig. 6 A.2). Therefore, this range of concentration readings would be indicative of 'no change' in leak conditions. By extension, deviations outside this window would be a cause for concern, stimulating action by the distribution company. In addition, the CH_4 concentrations measured by the sensors generally decreased as the distance from the leak increased (Fig. 6), although observed concentrations from more distant sensors could occasionally exceed those of the sensor directly over the leak. These changes were likely caused by changes in the environmental conditions, especially *RH*, temperature, and pressure, and wind speed. Consistent with previous findings [24], enhanced CH_4 concentration along the pipeline trenches buried at depths of 0.61 and 0.91 m was observed. Lower concentrations typically measured above the soil surface of the undisturbed soil implied a lower methane flux as expected due to the lower permeability of the undisturbed soil in the testbed. The CH_4 concentration distribution (Fig. S6) was similar with both

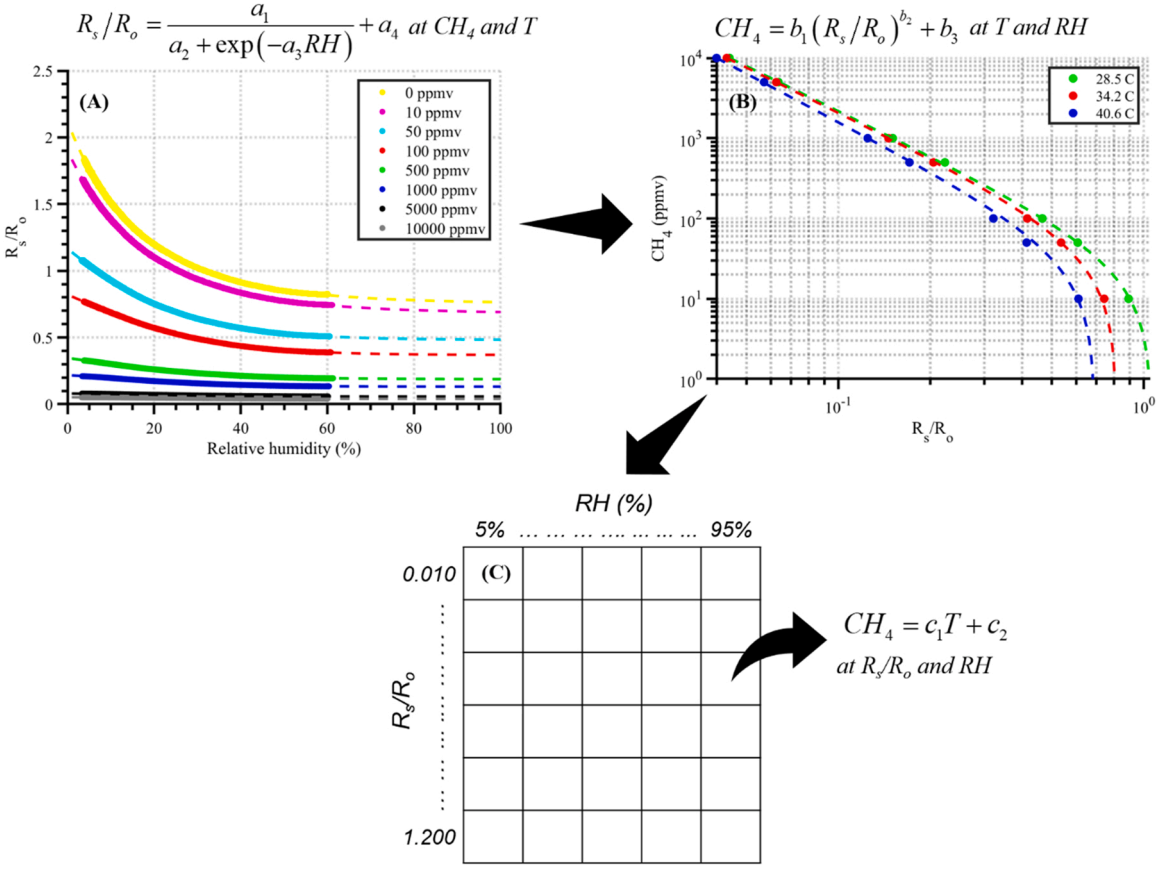

Fig. 4. . Illustration of the multivariate nonlinear regression processing of the sensor data. (A) Relationship between *RH* and R_s/R_o are characterized by sigmoid functions. (B) R_s/R_o is then correlated to CH_4 concentration using power functions for T= 28.5, 34.2, and 40.6 ℃. (C) A calibration table was then constructed to cover *RH* from 5% to 95% and R_s/R_o from 0.01 to 1.20. Correlations in the calibration table are polynomials as a function of air temperature. Coefficients of functional forms are listed in SI Appendix (Table S2 and S3).

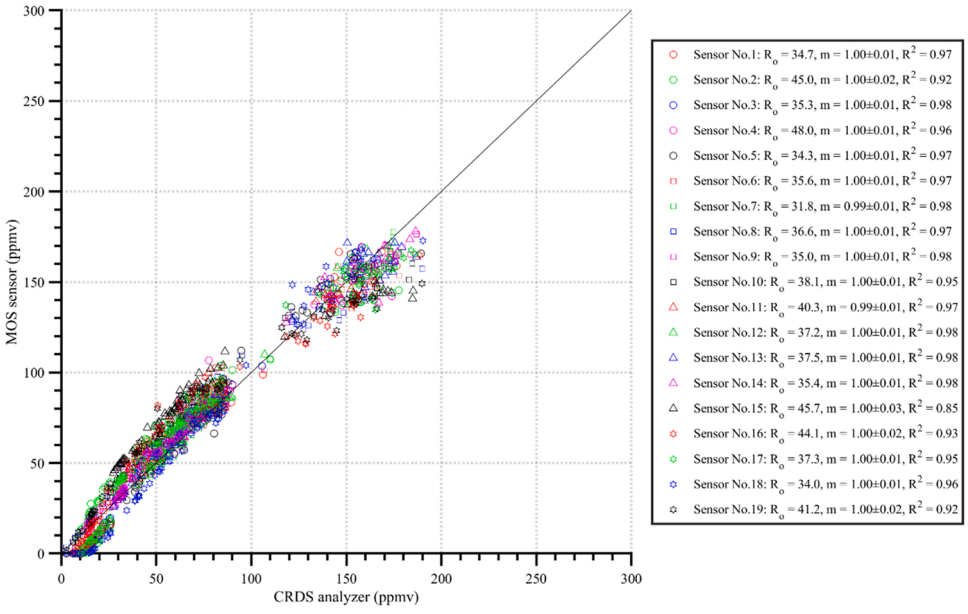

Fig. 5. . Comparison of 100-second averaged CH_4 concentrations from the MOS sensor and the CRDS analyzer. The adjusted R_o, m, and R^2 values estimated from linear regression for each LCS unit are listed. The black line represents the identity line (1:1 line).

experiments. The results suggest that the observed near surface plumes reflected subsurface structures.

The atmospheric conditions measured over the full 24-hour period indicate a clear, relatively consistent diurnal pattern (Fig. 7 A— D). The daytime wind speed (average of 2.21 ± 1.58 m s^{-1}) was slightly higher than was observed at nighttime (average of 2.18 ± 1.94 m s^{-1})

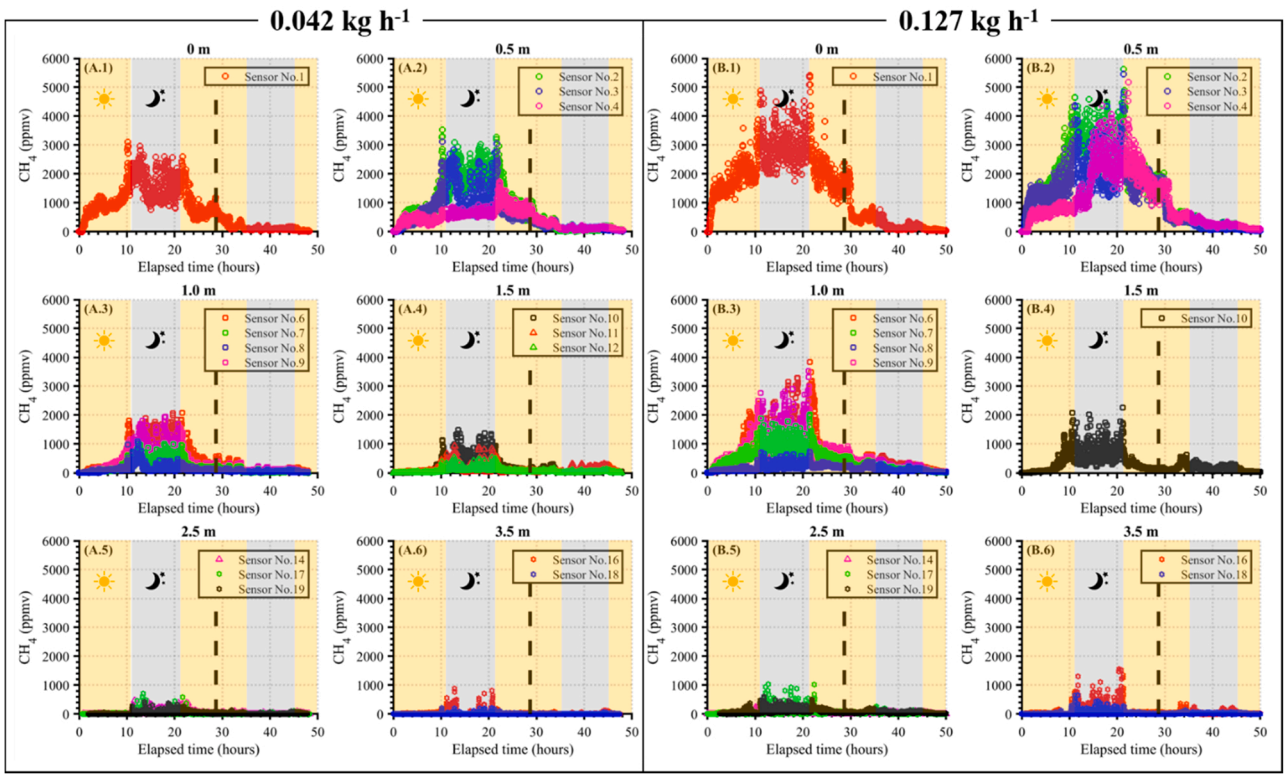

Fig. 6. . The time series of 100-second averaged CH_4 concentrations measured at multiple locations during 0.042 and 0.127 kg h^{-1} experiments (0 m is directly above the emission point). The corresponding distance from the emission point is labeled above each plot. The black dashed line represents the time of gas shutoff which is approximately 29 h from the release. The daytime (6 am—7 pm) and nighttime (7 pm—6 am) are illustrated by shaded areas.

(Fig. 7 A), while *RH* ranged from 11% to 95% over the measurement period. However, the diurnal variation of *RH* does not necessarily indicate change in the water vapor content of the atmosphere, as RH is strongly influenced by diurnal temperature variations [53]. absolute humidity (*AH*) remained essentially constant – 0.012 ± 0.003 kg/m^3 and 0.008 ± 0.002 kg/m^3 for the 0.042 and 0.127 kg h^{-1} experiments, respectively (Fig. S7).

In the 0.042 kg h^{-1} experiment, CH_4 concentrations of Sensor No. 1 at nighttime (averaging 1618 ± 468 ppmv) is clearly higher than in daytime (averaging 964 ± 474 ppmv) after quasi-steady state was achieved (Fig. 7E). A similar pattern was observed from all the LCS units (Fig. 6). Utilizing the period when the leak was in this quasi-steady state (i.e. 12—29 h after release started), the impact of meteorological parameters could be analyzed independently of changes in the subsurface leak characteristics (Fig. 8) for the purpose of capturing trends. Predominantly, increased wind speed resulted in decreased observed CH_4 concentration (Fig. 8 A.1 and B.1) while increased barometric pressure increased CH_4 concentration (Fig. 8 A.4 and B.4). When wind speed and direction were correlated with CH_4 concentration (Fig. S13), increased CH_4 concentration was observed in the downwind direction with wind speeds of 2—4 m s^{-1}. Under 2 m s^{-1} wind speed, regardless of wind direction, increased CH_4 concentration was seen up to 3.5 m from the leakage point.

Independent causation cannot be independently inferred as wind speed was correlated with pressure, temperature, and *RH*. To address this issue, a base regression model was developed in a rational function to predict CH_4 concentration using all meteorological parameters (Fig. S15). A multiple regression was performed by removing each meteorological parameter from the base model to evaluate its impact on measured CH_4 concentration (Fig. S16). Pressure and *RH* had the least substantial impacts (pressure up to 35%;*RH* 4%), indicating strong performance of the calibration method, which was expressly designed to minimize the impact of *RH* and, to a lesser extent, pressure, on the sensor outputs. In contrast, temperature and wind speed, which are correlated (R^2 of 0.41–0.59, Fig. S7) had higher impacts: temperature up to 176% on R^2 and 148% on root mean squared error (RMSE), and wind speed up to 143% on R^2 and 142% on RMSE.

These data indicate that the sensors respond to wind speed, which is known to substantially impact observed CH_4 concentrations, with robust rejection of changes in barometric pressure and *RH*, which are not expected to impact CH_4 concentrations. Therefore, the sensors have the correct characteristics to monitor subsurface leaks while characterizing near-surface meteorological impacts on gas movement and resulting concentration.

4. Discussion

Comparison of CH_4 concentration measured by the MOS sensor and the CRDS analyzer indicate that the MOS sensor can measure CH_4 concentrations in the 100—10,000 ppmv range seen when monitoring underground leaks. This study shows that, while the MOS sensor is rated for concentrations above 500 ppmv, proper calibration and real-time monitoring of environmental conditions provides usable performance down to 100 ppmv. Additionally, the overall response characteristics of the sensors can be identified by extensively calibrating a subset of sensors, and then adjusting the calibration of each TGS2611-E00 sensor by adjusting R_o, a parameter readily measured by using a high precision CH_4 instrument to acquire background CH_4 concentration. This indicates that a readily adaptable procedure could be implemented to periodically calibrate or qualify a large number of sensors at reasonable cost.

Since response time of the MOS sensor is slower than high speed analyzers, like the CRDS, measurements are more robust with averaging intervals in the 1-minute range, with 100-second averaging recommended for the sensors tested here. The observed differences in CH_4 concentration between the MOS and CRDS measurements, while non-

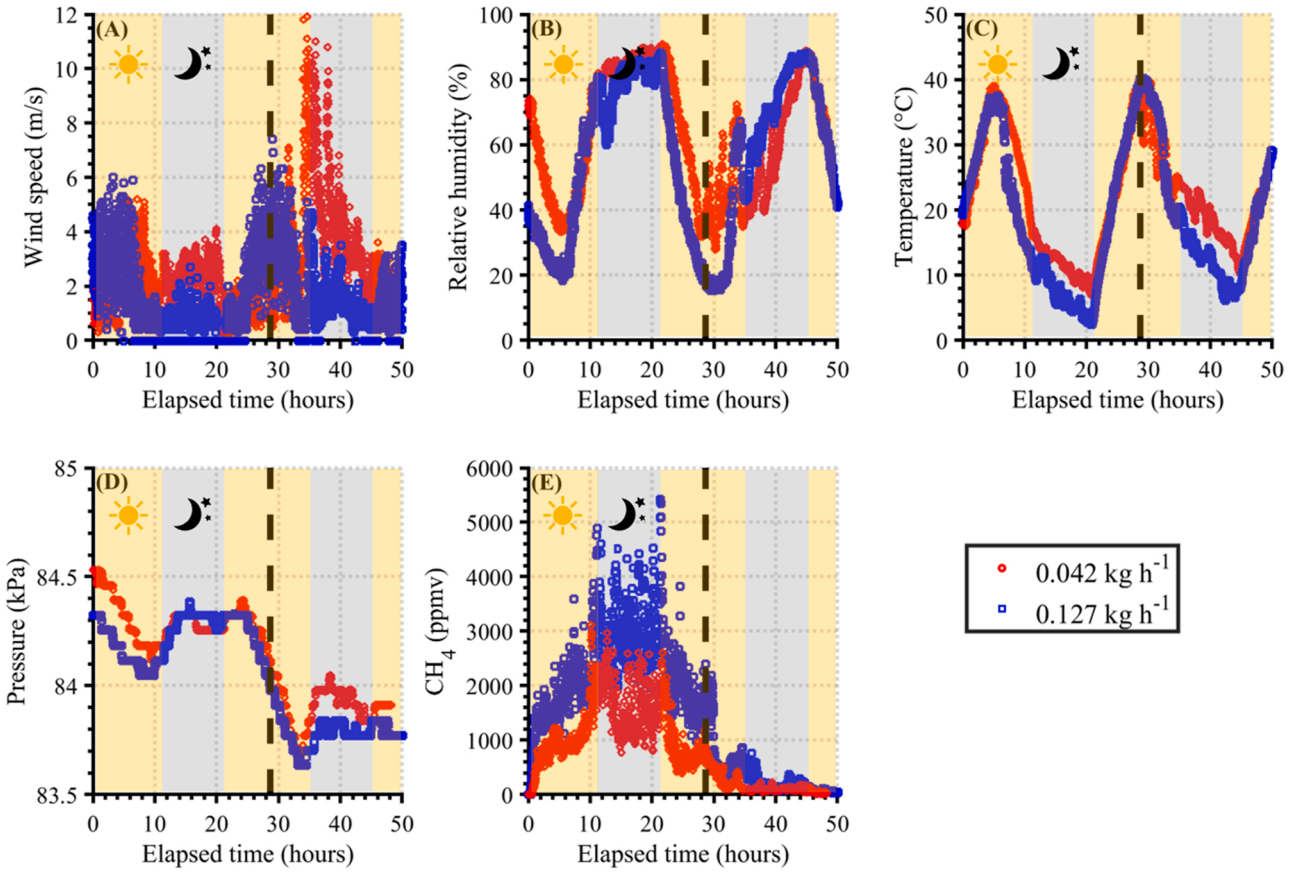

Fig. 7. . Panel A: Wind speed recorded 6 m above the ground. Panels B-D: Diurnal meteorological parameters of interest: (B) relative humidity, (C) air temperature, and (D) atmospheric pressure measured on Sensor No. 1. Panel E: Time series of 100-second averaged CH_4 concentrations measured from Sensor No. 1. Gas release and daytime markers as in Fig. 6.

trivial (19% on average) provide sufficient information for a long-term monitoring algorithm, using data from several properly positioned sensors, to surveil a known leak with sufficient confidence for the proposed application. Therefore, the combination of (a) extended operational range to 100 ppmv, (b) a manageable calibration procedure, and (c) sufficient accuracy for the application indicate that an inexpensive MOS sensor measure CH_4 concentrations reliably enough to detect changes in the emission state of an underground pipeline leak.

The above sensors must be combined with algorithms which would translate observed concentrations into actionable information for distribution companies. In the case of a known leak location, changes in concentrations over space and time can be monitored on a continuous basis by multiple sensors at lower cost than dispatching technicians to survey the leak periodically. Algorithms would then detect concentration levels or patterns that indicate a change in the leak condition, such as an increase in leak rate or increased gas migration distance, and signal follow-up action by the distribution company. When actual leak locations are unknown in field, the sensors could be installed in a network along the distribution pipelines, providing continuous monitoring and early detection over a wider area, for example an area with known pipeline issues, such as older, unprotected steel or cast iron, pipe. High resolution data could also be coupled to dispersion modeling to provide information comparable to periodic screening using high-precision analyzers to support comparison between driving survey increasingly deployed by distribution companies with results from these sensor networks.

Background concentration observed at the METEC was typically ~2 ppmv; however, due to the uncertainty in calibration (12 ppmv), the MOS sensors could not measure 1 ppmv accurately; as stated earlier, the calibration was effective from 100—10,000 ppmv. As a result, the CH_4 concentrations measured in the beginning of the 0.042 kg h^{-1} experiment was 0.1 ppmv, similarly observed in the 0.127 kg h^{-1} experiment. However, even 19 h after gas shut-off, the CH_4 concentration readings did not return to the background concentration. While below the calibration range, this offset suggests that the CH_4 stored in subsurface may contribute to near-surface CH_4 concentrations for substantial periods after a gas leak is stopped, even in sandy soil with relatively high permeability. With further exploration, these data indicate that similar sensors would be useful for monitoring leak venting after a leak is fixed – an ongoing and problematic area for industry.

Overall, this study shows that the data measured at high spatio-temporal resolution provides an effective monitoring option for the variability in gas concentrations due to environmental conditions. The general approach utilized here is the identification of variables affecting atmospheric CH_4 transport near the ground surface. Given the low cost of these sensors, and the ability to deploy the sensors for long periods directly on the ground, these sensors could also be used to investigate exchange of water, heat, and volatile organic compounds at land-atmosphere interface. Although the controlled experiments focus on relatively finer spatial scales, covering up to 3.5 m from the emission point, fundamental principles underlying gas transport near ground surface remain substantially intact regardless of scale.

5. Conclusion

We present development and calibration of a NG detection unit using low-cost sensors and field application of the units. A comparison of the MOS sensors used in the NG detection unit and CRDS analyzer was in a good agreement, demonstrating effectiveness of a universal calibration model developed in this study which accounts sensor-specific variation

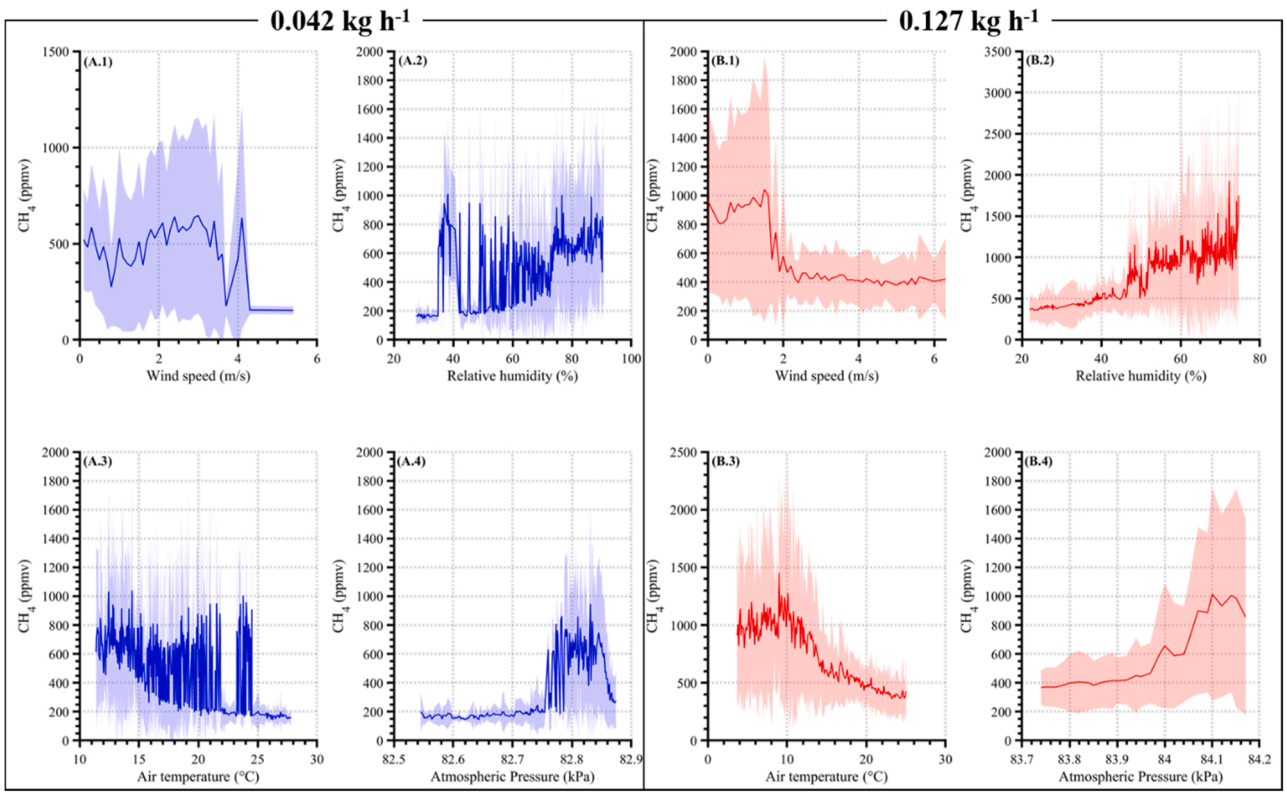

Fig. 8. . Effect of meteorological parameters measured from the meteorological station on averaged CH_4 concentration near the ground surface measured at 1.0 m away from the emission point during 0.042 kg h^{-1} (A.1—A.4) and 0.127 kg h^{-1} (B.1—B.4) experiments. The CH_4 concentrations measured 12–29 h after the release started were averaged by the corresponding meteorological values. The shaded area represents one standard deviation of the CH_4 concentration measured 1.0 m away from the emission point.

for measurements of CH_4 concentrations. In field experiments, the MOS sensor measured CH_4 concentrations reliable enough to detect changes in the emission state of an underground pipeline leak.

Current work practice in industry is to identify leaks, and, if a leak does not need to be fixed immediately for safety reasons, to monitor known leaks periodically (annual or biannual surveys are common) until repairs are completed. In many instances, leaks may remain unfixed for several years. This study illustrates that an alternative to periodic surveys may be possible. Specifically, an identified leak could be continuously surveilled by low-cost sensors, reporting in near real time, for an extended period. This method would reduce surveillance costs, while providing an earlier warning of potential safety risks.

While this study represents preliminary findings for this type of application, additional development and testing are required for practical applications, including improved sensor module designs, integration with communication and independent power, and development of supporting algorithms. Finally, the results presented here provide a framework to better understand variability in fugitive gas emissions from NG pipelines leaks, findings which could improve estimates of greenhouse gas emissions.

CRediT authorship contribution statement

Younki Cho: Conceptualization, Methodology, Software, Validation, Formal analysis, Writing – original draft, Writing – review & editing, Visualization. **Kathleen M. Smits**: Conceptualization, Funding acquisition, Methodology, Project administration, Resources, Supervision, Writing – review & editing. **Stuart N. Riddick**: Data curation, Methodology, Investigation, Writing – review & editing. **Daniel J. Zimmerle**: Funding acquisition, Methodology, Project administration, Resources, Writing – review & editing.

Declaration of Competing Interest

The authors declare that they have no known competing financial interests or personal relationships that could have appeared to influence the work reported in this paper.

Acknowledgements

This material is based upon work supported by the Department of Energy (DOE) Advanced Research Projects Agency-Energy (ARPA-E) Methane Observation Networks with Innovative Technology to Obtain Reductions (MONITOR) program, USA under Grant No. DE-FOA-0001546, the US Department of Transportation (DOT) Pipeline and Hazardous Materials Safety Administration (PHMSA), USA under Grant Nos. 693JK31810013 and 693JK32050005CAAP. The authors would also like to thank Clay Bell (Colorado State University) and Aidan Duggan (Colorado State University) for their expertise and assistance with field experiments at the METEC facility. Any opinion, findings, and conclusions or recommendations expressed herein are those of the authors and do not necessarily reflect the views of those providing technical input or financial support. The trade names mentioned herein are merely for identification purposes and do not constitute endorsement by any entity involved in this study.

Appendix A. Supporting information

Supplementary data associated with this article can be found in the online version at doi:10.1016/j.snb.2021.131276.

References

[1] J. Myhre, G. Shindell, D, Pongratz, Anthropogenic and natural radiative forcing, in: Clim. Chang. 2013 Phys. Sci. Basis Work. Gr. I Contrib. to Fifth Assess. Rep. Intergov. Panel Clim. Chang., Cambridge University Press, 2013, pp. 659–740, https://doi.org/10.1017/CBO9781107415324.018.

[2] IPCC, Climate Change, The Physical Science Basis. Contribution of Working Group I to the Fifth Assessment Report of the Intergovernmental Panel on Climate Change, Cambridge University Press, Cambridge, United Kingdom and New York, NY, USA, 2013, pp. 2013–2201.

[3] R.B. Jackson, M. Saunois, P. Bousquet, J.G. Canadell, B. Poulter, A.R. Stavert, P. Bergamaschi, Y. Niwa, A. Segers, A. Tsuruta, Increasing anthropogenic methane emissions arise equally from agricultural and fossil fuel sources, Environ. Res. Lett. 15 (2020), 071002, https://doi.org/10.1088/1748-9326/ab9ed2.

[4] National Academies of Sciences Engineering and Medicine, Improving Characterization of Anthropogenic Methane Emissions in the United States, The National Academies Press, Washington, DC, 2018.

[5] EPA, Inventory of U.S. Greenhouse Gas Emissions and Sinks: 1990–2018, 2020.

[6] T.N. Lavoie, P.B. Shepson, M.O.L. Cambaliza, B.H. Stirm, S. Conley, S. Mehrotra, I. C. Faloona, D. Lyon, Spatiotemporal variability of methane emissions at oil and natural gas operations in the eagle ford basin, Environ. Sci. Technol. 51 (2017) 8001–8009, https://doi.org/10.1021/acs.est.7b00814.

[7] T.L. Vaughn, C.S. Bell, C.K. Pickering, S. Schwietzke, G.A. Heath, G. Pétron, D. J. Zimmerle, R.C. Schnell, D. Nummedal, Temporal variability largely explains top-down/bottom-up difference in methane emission estimates from a natural gas production region, Proc. Natl. Acad. Sci. 115 (2018) 11712–11717, https://doi.org/10.1073/pnas.1805687115.

[8] D. Johnson, R. Heltzel, D. Oliver, Temporal variations in methane emissions from an unconventional well site, ACS Omega 4 (2019) 3708–3715, https://doi.org/10.1021/acsomega.8b03246.

[9] W.T. Honeycutt, M. Taehwan Kim, N.F. Tyler Ley, Materer, Sensor array for wireless remote monitoring of carbon dioxide and methane near carbon sequestration and oil recovery sites, RSC Adv. 11 (2021) 6972–6984, https://doi.org/10.1039/D0RA08593F.

[10] Z.D. Weller, J.R. Roscioli, W.C. Daube, B.K. Lamb, T.W. Ferrara, P.E. Brewer, J. C. von Fischer, Vehicle-based methane surveys for finding natural gas leaks and estimating their size: validation and uncertainty, Environ. Sci. Technol. 52 (2018) 11922–11930, https://doi.org/10.1021/acs.est.8b03135.

[11] J.C. von Fischer, D. Cooley, S. Chamberlain, A. Gaylord, C.J. Griebenow, S. P. Hamburg, J. Salo, R. Schumacher, D. Theobald, J. Ham, Rapid, vehicle-based identification of location and magnitude of urban natural gas pipeline leaks, Environ. Sci. Technol. 51 (2017) 4091–4099, https://doi.org/10.1021/acs.est.6b06095.

[12] B.K. Lamb, S.L. Edburg, T.W. Ferrara, T. Howard, M.R. Harrison, C.E. Kolb, A. Townsend-Small, W. Dyck, A. Possolo, J.R. Whetstone, Direct measurements show decreasing methane emissions from natural gas local distribution systems in the United States, Environ. Sci. Technol. 49 (2015) 5161–5169, https://doi.org/10.1021/es505116p.

[13] A. Collier-Oxandale, J.G. Casey, R. Piedrahita, J. Ortega, H. Halliday, J. Johnston, M.P. Hannigan, Assessing a low-cost methane sensor quantification system for use in complex rural and urban environments, Atmos. Meas. Tech. 11 (2018) 3569–3594, https://doi.org/10.5194/amt-11-3569-2018.

[14] W. Eugster, G.W. Kling, Performance of a low-cost methane sensor for ambient concentration measurements in preliminary studies, Atmos. Meas. Tech. 5 (2012) 1925–1934, https://doi.org/10.5194/amt-5-1925-2012.

[15] W. Eugster, J. Laundre, J. Eugster, G.W. Kling, Long-term reliability of the Figaro TGS 2600 solid-state methane sensor under low-Arctic conditions at Toolik Lake, Alaska, Atmos. Meas. Tech. 13 (2020) 2681–2695, https://doi.org/10.5194/amt-13-2681-2020.

[16] T. Aldhafeeri, M.-K. Tran, R. Vrolyk, M. Pope, M. Fowler, A review of methane gas detection sensors: recent developments and future perspectives, Inventions 5 (2020) 28, https://doi.org/10.3390/inventions5030028.

[17] M. Dosi, I. Lau, Y. Zhuang, D.S.A. Simakov, M.W. Fowler, M.A. Pope, Ultrasensitive electrochemical methane sensors based on solid polymer electrolyte-infused laser-induced graphene, ACS Appl. Mater. Interfaces 11 (2019) 6166–6173, https://doi.org/10.1021/acsami.8b22310.

[18] H. Wan, H. Yin, L. Lin, X. Zeng, A.J. Mason, Miniaturized planar room temperature ionic liquid electrochemical gas sensor for rapid multiple gas pollutants monitoring, Sens. Actuators B Chem. 255 (2018) 638–646, https://doi.org/10.1016/j.snb.2017.08.109.

[19] B. Szulczyński, J. Gębicki, Currently commercially available chemical sensors employed for detection of volatile organic compounds in outdoor and indoor air, Environments 4 (2017) 21, https://doi.org/10.3390/environments4010021.

[20] T.A. Fox, A.P. Ravikumar, C.H. Hugenholtz, D. Zimmerle, T.E. Barchyn, M. R. Johnson, D. Lyon, T. Taylor, A methane emissions reduction equivalence framework for alternative leak detection and repair programs, Elem. Sci. Anthropocene 7 (2019) 30, https://doi.org/10.1525/elementa.369.

[21] D. Bastviken, J. Nygren, J. Schenk, R. Parellada Massana, N.T. Duc, Technical note: facilitating the use of low-cost methane (CH_4) sensors in flux chambers – calibration, data processing, and an open-source make-it-yourself logger, Biogeosciences 17 (2020) 3659–3667, https://doi.org/10.5194/bg-17-3659-2020.

[22] M. van den Bossche, N.T. Rose, S.F.J.De Wekker, Potential of a low-cost gas sensor for atmospheric methane monitoring, Sens. Actuators B Chem. 238 (2017) 501–509, https://doi.org/10.1016/j.snb.2016.07.092.

[23] S.N. Riddick, D.L. Mauzerall, M. Celia, G. Allen, J. Pitt, M. Kang, J.C. Riddick, The calibration and deployment of a low-cost methane sensor, Atmos. Environ. 230 (2020), 117440, https://doi.org/10.1016/j.atmosenv.2020.117440.

[24] Y. Cho, B.A. Ulrich, D.J. Zimmerle, K.M. Smits, Estimating natural gas emissions from underground pipelines using surface concentration measurements, Environ. Pollut. 267 (2020), 115514, https://doi.org/10.1016/j.envpol.2020.115514.

[25] Railroad Commission of Texas, Chapter 8 Pipeline Safety Regulations Subchapter A General Requirements and Definitions, (2017). ⟨https://www.rrc.state.tx.us/media/42553/chapter8-all-effective-oct30–2017.pdf⟩ (accessed November 20, 2020).

[26] K.L. Smith, J.J. COLLS, M.D. Steven, A facility to investigate effects of elevated soil gas concentration on vegetation, 2005 1611, Water Air Soil Pollut. 161 (2005) 75–96, https://doi.org/10.1007/S11270-005-2833-X.

[27] H.Z. Li, M. Mundia-Howe, M.D. Reeder, N.J. Pekney, Gathering pipeline methane emissions in utica shale using an unmanned aerial vehicle and ground-based mobile sampling, 716, Atmos 2020 Vol. 11 (11) (2020) 716, https://doi.org/10.3390/ATMOS11070716.

[28] C.S. University, Energy Institute METEC, Energy Inst. METEC. (2020). ⟨https://energy.colostate.edu/metec/⟩.

[29] E.J. Zhang, C.C. Teng, T.G. van Kessel, L. Klein, R. Muralidhar, G. Wysocki, W.M. J. Green, Field deployment of a portable optical spectrometer for methane fugitive emissions monitoring on oil and gas well pads, Sensors 19 (2019) 2707, https://doi.org/10.3390/s19122707.

[30] C.J. Jørgensen, J. Mønster, K. Fuglsang, J.R. Christiansen, Continuous methane concentration measurements at the Greenland ice sheet-atmosphere interface using a low-cost, low-power metal oxide sensor system, Atmos. Meas. Tech. 13 (2020) 3319–3328, https://doi.org/10.5194/amt-13-3319-2020.

[31] Figaro, Technical information for TGS2611, 2012.

[32] J.D. Willey, G.B. Avery, J.D. Felix, R.J. Kieber, R.N. Mead, M.S. Shimizu, Rapidly increasing ethanol concentrations in rainwater and air, Npj Clim. Atmos. Sci. 2 (2019) 3, https://doi.org/10.1038/s41612-018-0059-z.

[33] R.J. Kieber, S. Tatum, J.D. Willey, G.B. Avery, R.N. Mead, Variability of ethanol and acetaldehyde concentrations in rainwater, Atmos. Environ. 84 (2014) 172–177, https://doi.org/10.1016/j.atmosenv.2013.11.038.

[34] G.B. Avery, L. Foley, A.L. Carroll, J.A. Roebuck, A. Guy, R.N. Mead, R.J. Kieber, J. D. Willey, S.A. Skrabal, J.D. Felix, K.M. Mullaugh, J.R. Helms, Surface waters as a sink and source of atmospheric gas phase ethanol, Chemosphere 144 (2016) 360–365, https://doi.org/10.1016/j.chemosphere.2015.08.080.

[35] J.D. Willey, J.P. Powell, G.B. Avery, R.J. Kieber, R.N. Mead, Use of experimentally determined Henry's Law and salting-out constants for ethanol in seawater for determination of the saturation state of ethanol in coastal waters, Chemosphere 182 (2017) 426–432, https://doi.org/10.1016/j.chemosphere.2017.05.044.

[36] V. Zgonnik, The occurrence and geoscience of natural hydrogen: a comprehensive review, Earth-Sci. Rev. 203 (2020), 103140, https://doi.org/10.1016/j.earscirev.2020.103140.

[37] P.C. Novelli, P.M. Lang, K.A. Masarie, D.F. Hurst, R. Myers, J.W. Elkins, Molecular hydrogen in the troposphere: Global distribution and budget, J. Geophys. Res. Atmos. 104 (1999) 30427–30444, https://doi.org/10.1029/1999JD900788.

[38] F.L. Conley, R.L. Thomas, B.L. Wilson, Measurement of volatile organic compounds in the urban atmosphere of Harris County, Texas, J. Environ. Sci. Heal. Part A. 40 (2005) 1689–1699, https://doi.org/10.1081/ESE-200067996.

[39] J.B. Gilman, B.M. Lerner, W.C. Kuster, J.A. de Gouw, Source signature of volatile organic compounds from oil and natural gas operations in Northeastern Colorado, Environ. Sci. Technol. 47 (2013) 1297–1305, https://doi.org/10.1021/es304119a.

[40] D. Helmig, C.R. Thompson, J. Evans, P. Boylan, J. Hueber, J.-H. Park, Highly elevated atmospheric levels of volatile organic compounds in the Uintah Basin, Utah, Environ. Sci. Technol. 48 (2014) 4707–4715, https://doi.org/10.1021/es405046r.

[41] Handbook of Natural Gas Transmission and Processing, Elsevier, 2015. ⟨https://linkinghub.elsevier.com/retrieve/pii/C20130156255⟩.

[42] Sensirion, Datasheet SHT3x-DIS Humidity and Temperature Sensor, 2019.

[43] E.F. Aghdam, C. Scheutz, P. Kjeldsen, Impact of meteorological parameters on extracted landfill gas composition and flow, Waste Manag. 87 (2019) 905–914, https://doi.org/10.1016/j.wasman.2018.01.045.

[44] L. Xu, X. Lin, J. Amen, K. Welding, D. McDermitt, Impact of changes in barometric pressure on landfill methane emission, Glob. Biogeochem. Cycles 28 (2014) 679–695, https://doi.org/10.1002/2013GB004571.

[45] STMicroelectronics, LPS25HB Datasheet, 2016.

[46] M. Technology inc., megaAVR Data Sheet, 2018.

[47] Colorado State University, Christman Field Observations, (2017). ⟨https://www.atmos.colostate.edu/fccwx/fccwx_latest.php⟩.

[48] Vaisala, HMP7 Relative Humidity and Temperature Probe, 2019.

[49] M. Mitton, Subsurface methane migration from natural gas distribution pipelines as affected by soil heterogeneity: field scale experimental and numerical study, Colo. Sch. Mines. Arthur. Lakes Libr. (2018). ⟨https://mountainscholar.org/handle/11124/172530⟩.

[50] B.A. Ulrich, M. Mitton, E. Lachenmeyer, A. Hecobian, D. Zimmerle, K.M. Smits, Natural gas emissions from underground pipelines and implications for leak detection, Environ. Sci. Technol. Lett. 6 (2019) 401–406, https://doi.org/10.1021/acs.estlett.9b00291.

[51] D.J. Zimmerle, C.K. Pickering, C.S. Bell, G.A. Heath, D. Nummedal, G. Pétron, T. L. Vaughn, Gathering pipeline methane emissions in Fayetteville shale pipelines

and scoping guidelines for future pipeline measurement campaigns, Elementa 5 (2017), https://doi.org/10.1525/elementa.258.
[52] B.K. Lamb, M.O.L. Cambaliza, K.J. Davis, S.L. Edburg, T.W. Ferrara, C. Floerchinger, A.M.F. Heimburger, S. Herndon, T. Lauvaux, T. Lavoie, D.R. Lyon, N. Miles, K.R. Prasad, S. Richardson, J.R. Roscioli, O.E. Salmon, P.B. Shepson, B. H. Stirm, J. Whetstone, Direct and indirect measurements and modeling of methane emissions in Indianapolis, Indiana, Environ. Sci. Technol. 50 (2016) 8910–8917, https://doi.org/10.1021/acs.est.6b01198.
[53] I. Moradi, P. Arkin, R. Ferraro, P. Eriksson, E. Fetzer, Diurnal variation of tropospheric relative humidity in tropical regions, Atmos. Chem. Phys. 16 (2016) 6913–6929, https://doi.org/10.5194/acp-16-6913-2016.

Younki Cho is a postdoctoral researcher in the department of Civil Engineering at the University of Texas at Arlington. He received his Ph.D. from the Colorado School of Mines. His research interests focus on multiphase fluid flow in porous media and its application in the areas of energy and environment.

Kathleen M. Smits is an Associate Professor in the department of Civil Engineering at the University of Texas at Arlington. She specializes in the study of gas transport and release from porous media. Her research uses a combination of experiments and mathematical models to address questions pertinent to both energy and the environment. She received her B.S. from the U.S. Air Force Academy, M.S. from the University of Texas, Austin, and PhD from Colorado School of Mines.

Stuart N. Riddick is a research scientist at the Energy Institute at Colorado State University. He received his BSc from the University of St. Andrews and PhD from King's College London. His research focuses on improving the understanding of the impact of trace gases on climate change and the potential for better control by the energy, waste and agriculture sectors.

Daniel J. Zimmerle is the Director of the Methane Emissions Program in the Energy Institute at Colorado State University. He was a principal investigator on four major studies of methane emissions in the natural gas supply chain, including studies of upstream, midstream, and distribution systems at a nation and/or regional scale, and leads the Methane Emissions Technology Evaluation Center, one of the largest test facilities for natural gas leak detection solutions. His current research on natural gas emissions includes studies of equipment and pipeline emissions, field studies, and fundamental investigations of commonly utilized several leak detection and quantification methods, including optical gas imaging (OGI), high flow sampling, and downwind methods.